Quantum spin model of a cubic ferromagnet in a magnetic field

M. Dudziński[1,2,a], J. Sznajd[2], and J. Zittartz[1]

[1] Institut für Theoretische Physik, Universität zu Köln, 50937 Köln, Germany
[2] Institute for Low Temperature and Structure Research, Polish Academy of Sciences, P.O. Box 1410, 50-950 Wroclaw 2, Poland

Abstract. The zero temperature phase diagram of a one-dimensional ferromagnet with cubic single ion anisotropy in an external magnetic field is studied. The mean-field approximation and the density-matrix renormalization group method are applied. Two phases at finite magnetic fields are identified: a canted phase with spontaneously broken symmetry and a phase with magnetization along the magnetic field. Both methods predict that the canted phase exists even for the single-ion anisotropy strong enough to destroy the magnetic order at zero magnetic field. In contrast to the mean-field theory, the density-matrix renormalization group predicts a reentrant behavior for the model. The character of the phase transition at finite magnetic field has also been considered and the critical index $\beta_c = 1/8$ has been found.

1 Introduction

Magnetic ordering in ferromagnets with cubic crystal field is an old topic which has been studied for decades [1]. There are basically two possible approaches. In the first one, which is suitable for explaining critical behavior, one works with a phenomenological Landau-Ginzburg-Wilson Hamiltonian. In recent years, the question whether the cubic fixed point is stable in three dimensions has been a subject of intensive research [2–5].

However, to establish theoretically the *existence* of different phases one must work with a microscopic quantum Hamiltonian. In the present paper we are interested in this second approach. We emphasize that the investigation of quantum spin Hamiltonians with cubic single-ion anisotropy poses a considerable problem for the following two reasons. Firstly, one must take $S \geq 2$, otherwise the crystal-field term becomes trivial. The large number of possible states per site is an obvious difficulty. Secondly, as the cubic crystal field breaks the continuous rotational symmetry of the model, there are no simple conserved quantities like S^z. In consequence, only the mean field approximation (MFA) has been usually applied to these models [6–9]. As is well known, the MFA neglects fluctuations, and the natural question arises whether the phase diagrams of cubic ferromagnets would change qualitatively, if the fluctuations were taken into account in some more sophisticated theory.

In our recent papers, we have studied a model of a three-axial cubic ferromagnet with smallest nontrivial

a e-mail: md@thp.uni-koeln.de

$S = 2$, applying perturbation theory [10], density-matrix renormalization group [11], and real-space renormalization ideas [12]. The most important conclusion was that in addition to the possible phases obtained in the MFA (magnetic and disordered), a completely new, quadrupolarly ordered phase appeared when the quantum fluctuations were not neglected in the theory. This result is valid for the model in one, two, and three dimensions, and it shows that the MFA can be qualitatively wrong in all these cases.

In the present work, we study the above mentioned $S = 2$ quantum ferromagnet in an externally applied magnetic field. The focus is on the different phases and spontaneous symmetry breaking in the ground state. The model is specified in Section 2. Section 3 contains the appropriate mean field treatment, while the detailed MFA-calculations are deferred to the Appendix. In Section 4, calculations for the one-dimensional model are performed using the density-matrix renormalization group method (DMRG), and a comparison with the MFA results is made. Section 5 contains our conclusions.

2 The model

In a three-axial cubic ferromagnet, the spontaneous magnetization has six possible orientations parallel to directions [100], [010], [001]. Consider now what happens when a magnetic field is applied. For general field direction, no particular symmetry is left and we expect no spontaneous symmetry breaking. If, however, the field is applied along a high-symmetry axis like [101] or [111], then spontaneous symmetry breaking is still possible. Thus, these two field

Fig. 1. The two expected situations at finite magnetic fields: (a) broken symmetry in the canted phase and $m^\perp \neq 0$, (b) magnetization along the field and $m^\perp = 0$ in the second phase.

directions are most interesting, if we want to investigate phase transitions.

In the case when the magnetic field is directed along the [111] axis, the spontaneous magnetization may have three possible positions. Unfortunately, we were not able to carry out reliable numerical investigations for this situation. We encountered numerical instabilities in the Lanczos diagonalization procedure, and also the precision of the DMRG method itself was not sufficient. Therefore, here we consider only the case where the magnetic field is directed along the [101] axis, which case turned out to be tractable.

The model Hamiltonian is the following

$$H = -\sum_{(ij)} (\mathbf{S}_i \mathbf{S}_j) - D \sum_i \left[(S_i^x)^4 + (S_i^y)^4 + (S_i^z)^4 \right]$$
$$-h \sum_i \frac{1}{\sqrt{2}} (S_i^x + S_i^z), \tag{1}$$

where the spin operators for $S = 2$ are denoted by S_i^α. The first term is the ferromagnetic coupling between nearest neighbors; the second term describes the cubic crystal field which for $D > 0$ favors the directions [100], [010], and [001], for spontaneous ordering (three-axial ferromagnet). Finally, the third term is the externally applied magnetic field in the direction [101]. Our aim is to obtain the zero-temperature phase diagram for this model.

Taking into account that for $h = 0$ the model (1) is a three-axial ferromagnet, one can expect that two phases should exist at finite field h. In the first phase, with spontaneously broken symmetry, the magnetization should have two possible positions in the XZ plane, and in the second phase the magnetization should be parallel to the field direction (Fig. 1). The order parameter which distinguishes between the two phases is the magnetization component perpendicular to the magnetic field

$$m^\perp = \frac{1}{\sqrt{2}} (m^z - m^x), \tag{2}$$

and we define the parallel component as

$$m = \frac{1}{\sqrt{2}} (m^z + m^x) \tag{3}$$
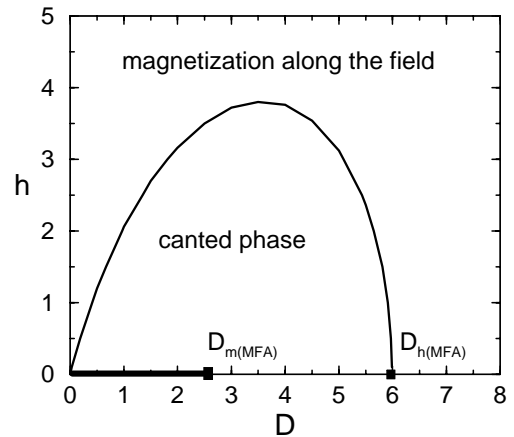
Fig. 2. The mean-field phase diagram of the model.

where

$$m^\alpha = \langle S_i^\alpha \rangle, \qquad \alpha = x, y, z. \tag{4}$$

In the phase with broken symmetry, which will be called *canted phase*, we have $m^\perp \neq 0$, and in the second phase $m^\perp = 0$.

3 The MFA treatment

For the model (1) the single-site MFA Hamiltonian reads

$$H_{\mathrm{MFA}} = \frac{z}{2} \mathbf{m}^2 - z\mathbf{m}\mathbf{S} - D \left[(S^x)^4 + (S^y)^4 + (S^z)^4 \right]$$
$$-h \frac{1}{\sqrt{2}} (S^x + S^z), \tag{5}$$

where z denotes the number of nearest neighbors. In what follows, we set $z = 2$ for a convenient comparison with the results of the one-dimensional case. The MFA solution is found by minimizing the ground-state energy E_0 of the Hamiltonian (5) with respect to the variational parameters m^α. The MFA calculations are contained in the Appendix and the MFA phase diagram is shown in Figure 2. At $h = 0$, we have a spontaneous magnetization (in X, Y, or Z-direction) for $0 \leq D \leq D_{\mathrm{m(MFA)}} = \frac{8}{3}$, given by (A.3). The ordered phase is 6-fold degenerate, above $\frac{8}{3}$ we have the disordered phase.

As explained in the Appendix, with $h \neq 0$ pointing in the [101] direction (Fig. 1) we have $m^y = 0$ and $m^z \geq m^x \geq 0$ (for convenience). One has to find the smallest eigenvalue E_0 of (5) and then one has to minimize this quantity with respect to m and $m^\perp$ (or m^z, m^x according to Eqs. (2, 3)). In the general case we have to deal with the 5-order characteristic polynomial (A.7) and the above procedure can be done only numerically. As a result we obtain the phase diagram (Fig. 2) and the order parameter $m^\perp$ for some D-values (Fig. 3).

However, for $D \geq \frac{8}{3}$ and small magnetic field ($h \to 0$) the above procedure can be performed analytically. The smallest eigenvalue E_0 is given by (A.9) and
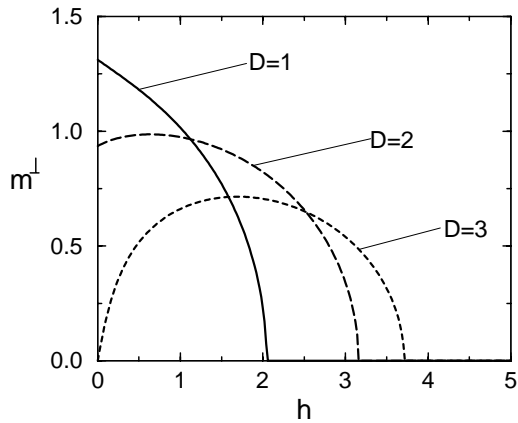
Fig. 3. The dependence of the order parameter $m^\perp$ on the magnetic field h for some chosen crystal fields D (MFA results.)

Fig. 4. The phase diagram in one dimension obtained by the density-matrix renormalization group method.

the minimization with respect to m and $m^\perp$ leads to equations (A.10, A.11), respectively. These results show that the phase boundary for $h \to 0$ ends at the exact value $D_{\mathrm{h[MFA]}} = 6$ (which checks very well with the numerics).

It is interesting to observe that the canted phase near $h = 0$ extends further than the 6-fold degenerate ordered phase at $h = 0$. We also note that at $h = 0$ the eigenvalue E_0 passes through $D_{\mathrm{h[MFA]}} = 6$ *without* singularity.

The canted phase is 2-fold degenerate (namely the Z_2-symmetry $X \leftrightarrow Z$ is broken) and at the phase boundary the transition is to the unique disordered phase. Such a $(2 \to 1)$ transition is in the universality class of the one-dimensional Ising model in a transverse field. Within MFA we have the characteristic square-root behavior $(\beta_{\mathrm{MFA}} = \frac{1}{2})$ of the order parameter. The exact transition, however, should have the critical exponent $\beta_{\mathrm{c}} = \frac{1}{8}$. The numerical results of the next section will indeed confirm this expectation.

4 The DMRG study in one dimension

The purpose of the present section is to verify the above MFA predictions by performing DMRG calculations in one dimension, where quantum fluctuations are strong. Note, that for a model without continuous rotational symmetry like our model (1), conventional long-range order in the ground state is possible even in one dimension.

The detailed description of the DMRG method can be found in the original papers by White [13]. The method allows to calculate low-lying eigenstates of long, but finite, quantum chains. Usually, systems with open boundary conditions are studied in practical applications, because the precision in this case is much better than for periodic boundary conditions.

Our aim is to calculate the order parameter $m^\perp$, whose nonzero values result from spontaneous symmetry breaking. To obtain such a quantity in a finite chain, we apply symmetry breaking boundary conditions. Namely, we apply an auxiliary magnetic field to the first and the last spin in the chain, so as to select one of the two possible
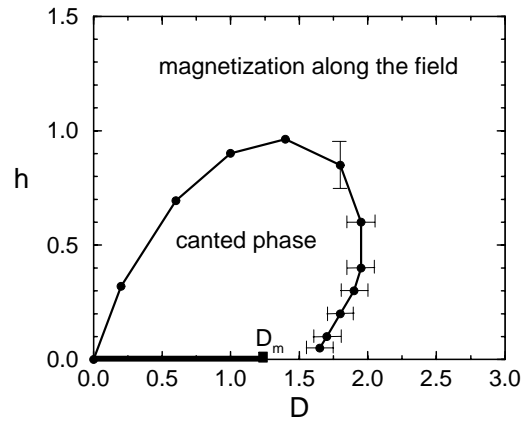
values of $m^\perp$. Provided that the chain length exceeds the appropriate correlation length many times, the bulk value of $m^\perp$ is observed in the middle part of the chain. Usually the bulk value is approached from above for strong auxiliary fields, and from below for weak auxiliary fields, which gives a convenient way to estimate errors. Such calculations have been described in detail in reference [11].

The above method does have limitations. Most importantly, when the correlation length is very large, it may turn out that the sufficient system size is beyond the computer capacity. Also, the large number of states per site in our model (1) and the lack of S^z conservation make the DMRG calculations difficult, and it may turn out that the DMRG itself is not precise enough in some areas in the (D, h) plane. (The DMRG precision strongly depends on the spectral properties of the Hamiltonian.)

In order to establish the ground-state phase diagram in one dimension, we have performed DMRG calculations for different (D, h) points. At finite magnetic fields, the same two phases as in the MFA have been identified: the canted phase with $m^\perp \neq 0$ and the phase with $m^\perp = 0$. The obtained phase diagram is shown in Figure 4, and it should be compared with the MFA phase diagram in Figure 2.

Let us now discuss in detail the features of the DMRG phase diagram. It has been obtained in reference [11] that the spontaneous magnetization along directions [100], [010], or [001] exists for $0 < D < D_{\mathrm{m}}$, with $D_{\mathrm{m}} = 1.2374(4)$. Similarly as in the MFA picture, also here the canted phase with $m^\perp \neq 0$ extends further, for larger D.

In Figure 5 we show the dependence of the order parameter $m^\perp$ on the magnetic field h for some values of the crystal-field parameter D. In order to obtain these curves we kept up to $M = 70$ states in the finite-system DMRG algorithm, and considered chains up to $L = 600$ sites long, which allowed us to calculate $m^\perp$ with uncertainties around 10^{-5}. Very close to the transition line between the two phases, the correlation length is very large, and the curves in Figure 5 could not be calculated further. Although it cannot be checked directly whether the transition is continuous or discontinuous, the large correlation
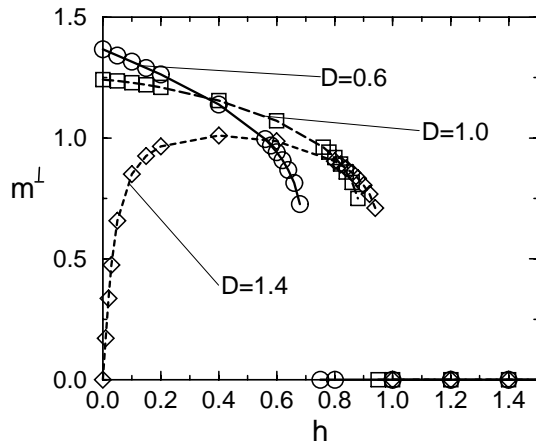
Fig. 5. The dependence of the order parameter $m^\perp$ on the magnetic field h for some chosen crystal fields D (DMRG results.)

Table 1. The results of the fitting analysis of the phase transition at finite magnetic fields.

D	h_c	β_c
0.2	0.320(2)	0.130(25)
0.6	0.694(2)	0.127(3)
1.0	0.901(1)	0.126(2)
1.4	0.963(2)	0.126(6)

lengths strongly suggest the former possibility. Therefore we analyze the above dependencies assuming the following power law for the order parameter

$$m^\perp = a(h_c - h)^{\beta_c} \tag{6}$$

where the parameter D is kept fixed. Good agreement with the assumption is found, and the results of the fitting analysis for a few different D values are presented in Table 1. The obtained critical exponent is always close to the value $\beta_c = 1/8$. This has been expected from the discussion at the end of the last section.

For larger D values ($D \geq 1.5$), the numerical calculations become more difficult. Firstly, the number of iterations in the Lanczos diagonalization procedure significantly increases, and secondly, the DMRG precision for a given M gets worse. In this region of the phase diagram we kept up to $M = 100$ states, which enabled us to study systems of about $L = 200$ sites. These system sizes were not sufficient to obtain precise estimates of $m^\perp$ so close to the phase-transition line that a similar fitting analysis as described above could be performed. We could only find bounds on the location of the phase-transition line, which are indicated in Figure 4. These bounds are firm, and they allow us to establish a major qualitative difference between the DMRG phase diagram and the MFA phase diagram. Namely, a reentrant behavior is observed in the DMRG picture, in contrast to the MFA theory.

The critical line cannot be traced down to $h = 0$ because of computational difficulties related mainly to the

fact that the order parameter $m^\perp$ is very small for small fields h. Nevertheless, it is seen in Figure 4 that, most probably, the line reaches the $h = 0$ axis at some finite $D_h \approx 1.6$. In particular, the possibility that it could end at the point D_m seems to be refuted, because for $D_m < D < D_h$ the dependence of $m^\perp$ on h is linear for small h.

Lastly we want to mention that the numerically exact DMRG results show that the areas of the ordered phases shrink as compared to the MFA-results. So the point D_m diminishes from $8/3$ to 1.2374 and the point D_h from 6 to ≈ 1.6. This is due to the fact that the MFA-theory neglects quantum fluctuations.

5 Conclusions

The ground state of the model in equation (1) has been studied using first the mean-field approximation and then the density-matrix renormalization group method. The main purpose was to examine using the DMRG whether there are qualitative changes to the MFA phase diagram when quantum fluctuations are no longer neglected.

We have found that the main qualitative features of the MFA phase diagram remain valid. Namely, in the DMRG picture the finite-field phase transition is also of second order, and the broken-symmetry canted phase exists also for those D values for which the magnetic order at zero magnetic field is already destroyed. The new feature is the appearance of the reentrant behavior.

Finally, for the finite-field phase transition we have found the critical exponent $\beta_c = \frac{1}{8}$, as expected.

Appendix

The single-site Hamiltonian (5) is diagonalized in the 5-dimensional space spanned by the eigenstates of the D-term. These are (S^z diagonal)

$$\begin{aligned}
\phi_1 &= |\,0\rangle, \\
\phi_2 &= \frac{1}{\sqrt{2}}(|\,2\rangle + |\,-2\rangle), \\
\phi_3 &= \frac{1}{\sqrt{2}}(|\,2\rangle - |\,-2\rangle), \\
\phi_4 &= |\,1\rangle, \\
\phi_5 &= |\,-1\rangle, \tag{A.1}
\end{aligned}$$

with D-eigenvalues: $E_1^0 = E_2^0 = -24D$, $E_3^0 = E_4^0 = E_5^0 = -18D$.

(a) First we consider $h = 0$ which case has been treated already in [8,11]. Spontaneous magnetization is expected in X, Y, or Z-direction. We choose the Z-direction, thus

$m^x = m^y = 0$, $m^z \neq 0$. Only the ϕ_2, ϕ_3 states couple and produce the smallest eigenvalue

$$E_0 = (m^z)^2 - 21D - \sqrt{9D^2 + 16(m^z)^2}. \qquad (A.2)$$

Minimization with respect to m^z leads to

$$m^z = 2\sqrt{1 - \left(\frac{3}{8}D\right)^2}, \qquad E_0 = -21D - 4 - \frac{9}{16}D^2 \qquad (A.3)$$

for $D \leq \frac{8}{3}$ and

$$m^z = 0, \quad E_0 = -24D \qquad (A.4)$$

for $D \geq \frac{8}{3}$. Therefore, at $h = 0$ we have the 6-fold degenerate ordered phase for $D \leq \frac{8}{3}$, the disordered phase for $D \geq \frac{8}{3}$. Further discussion is contained in [11].

(b) $h > 0$: the magnetic field forces **m** into the X, Z-plane, thus $m^y = 0$. h favors $m^z = m^x$ (≥ 0), but the D-term prefers either m^z or m^x, thus breaking the $X \leftrightarrow Z$ symmetry. We choose $m^z \geq m^x \geq 0$ and write (according to Eqs. (2, 3))

$$E = m^2 + (m^\perp)^2 - 24D - \varepsilon. \qquad (A.5)$$

The Hamiltonian matrix $\mathcal{M} = H_{\text{MFA}} - E\mathcal{I}$ is then

$$\mathcal{M} = \begin{bmatrix} \varepsilon & 0 & 0 & -\sqrt{3}\alpha & -\sqrt{3}\alpha \\ 0 & \varepsilon & -2\alpha_3 & -\alpha & -\alpha \\ 0 & -2\alpha_3 & 6D+\varepsilon & -\alpha & \alpha \\ -\sqrt{3}\alpha & -\alpha & -\alpha & 6D+\varepsilon-\alpha_3 & 0 \\ -\sqrt{3}\alpha & -\alpha & \alpha & 0 & 6D+\varepsilon+\alpha_3 \end{bmatrix} \qquad (A.6)$$

in terms of $\alpha = \frac{1}{2}h + \sqrt{2}m^x$, $\alpha_3 = \frac{1}{\sqrt{2}}h + 2m^z$. The eigenvalues ε (or E) result from $0 = \det \mathcal{M}$ which is a 5th order polynomial given by

$$0 = \varepsilon^2(6D + \varepsilon)^3 + 4\varepsilon\beta^4(1 + \gamma)^2 + 18D\beta^4(1 - \gamma)^2$$
$$-\varepsilon\beta^2(1 + \gamma)(6D + \varepsilon)(24D + 5\varepsilon) \qquad (A.7)$$

with more convenient parameters

$$\beta = h + 2m, \qquad \sqrt{\gamma} = \frac{2m^\perp}{\beta}, \qquad (0 \leq \gamma \leq 1) \qquad (A.8)$$

such that $\alpha_3 = \frac{1}{\sqrt{2}}\beta(1 + \sqrt{\gamma})$, $\alpha = \frac{1}{2}\beta(1 - \sqrt{\gamma})$. Obviously $\sqrt{\gamma}$ ranges in $(0, 1)$. The largest solution ε_0 must be substituted into (A.5) and then E_0 must be minimized with respect to $m^\perp$ and m.

In the general case (A.7) does not factor and the treatment must be done numerically resulting in the plots of Figures 2,3. An analytic treatment is possible for $D \geq D_{\text{m(MFA)}} \equiv \frac{8}{3}$ and small field h, where both m and $m^\perp$ are small of order h. Obviously $\varepsilon = O(h^2)$. Expanding (A.7) in h one obtains ε_0 which, substituted into (A.5), leads to

$$E_0 = -24D + m^2 + (m^\perp)^2$$
$$-\frac{\beta^2}{6D}\left[2(1 + \gamma) + \sqrt{1 + 14\gamma + \gamma^2}\right]. \qquad (A.9)$$

The variation with respect to $m^\perp$ gives

$$m^\perp = 0 \qquad \text{or} \qquad \frac{3}{2}D = 2 + \frac{7 + \gamma}{\sqrt{1 + 14\gamma + \gamma^2}}, \qquad (A.10)$$

resulting in $\gamma = \gamma(D)$. At $D = \frac{8}{3}$, $\gamma \nearrow 1$ which implies $\frac{m^x}{m^z} \to 0$, $\frac{h}{m^z} \to 0$. This means that $m^z = Ah + O(h^3)$ leads to $A \to \infty$ as $D \searrow \frac{8}{3}$, marking the onset of spontaneous magnetization at $h = 0$ (discussed before).

As D increases, γ decreases to zero precisely at $D \equiv D_{\text{h(MFA)}} = 6$. For $D \geq 6$ we have the trivial solution $m^\perp = 0$ (see Fig. 2).

The variation with respect to m results in

$$3D\frac{m}{h + 2m} = 2 + \frac{1 + 7\gamma}{\sqrt{1 + 14\gamma + \gamma^2}}. \qquad (A.11)$$

This checks with the discussion of (A.10) for $D \to \frac{8}{3}$. As D increases, $\gamma \to 0$ at $D = 6$. For all $D \geq 6$ we have from (A.11): $m = (D - 2)^{-1}h + O(h^3)$.

Finally for $D \approx 6$ and small h one can expand (A.10, A.11) to lowest order in γ which leads to

$$m^\perp = \frac{D}{8\sqrt{2}(D - 2)}\sqrt{6 - D}\, h, \qquad (A.12)$$

which square-root behavior is a typical MFA-result.

Lastly we mention that at $h = 0$ we have $m = m^\perp = 0$ for $D > \frac{8}{3}$. Therefore E_0 passes through $D = 6$ *without* singularity.

References

1. D. Mukamel, M.E. Fisher, E. Domany, Phys. Rev. Lett. **37**, 565 (1976), and references therein.
2. H. Kleinert, S. Thoms, V. Schulte-Frohlinde, Phys. Rev. B **56**, 14428 (1997).
3. J.M. Carmona, A. Pelissetto, E. Vicari, Phys. Rev. B **61**, 15136 (2000).
4. R. Folk, Yu. Holovatch, T. Yavors'kii, cond-mat/0003216.
5. A. Aharony, in *Phase Transitions and Critical Phenomena*, edited by C. Domb, M.S. Green (Academic, New York, 1976), Vol. 6.
6. J. Sznajd, J. Magn. Magn. Mater. **42**, 269 (1984).
7. V.V. Valkov, T.A. Valkova, Teor. Mat. Phys. **59**, 263 (1984).
8. A.I. Mitsek, K.Y. Guslienko, S.V. Pavlovskii, Phys. Stat. Sol. (b) **135**, 173 (1986).
9. Z. Domański, J. Sznajd, Phys. Stat. Sol. (b) **129**, 135 (1985).
10. M. Dudziński, J. Sznajd, Eur. Phys. J. B **5**, 745 (1998).
11. M. Dudziński, G. Fáth, J. Sznajd, Phys. Rev. B **59**, 13764 (1999).
12. J. Sznajd, M. Dudziński, Phys. Rev. B **59**, 4176 (1999).
13. S.R. White, Phys. Rev. Lett. **69**, 2863 (1992); S.R. White, Phys. Rev. B **48**, 10345 (1993).